

## **Weld Toe Stress Concentrations in Multi Planar Stiffened Tubular KK Joints**

C. O. Woghiren<sup>1, a</sup> and F. P. Brennan<sup>2, b</sup>

<sup>1</sup>Mobil Producing Nigeria Unlimited, Room 6B 28A, Mobil House, Lagos, Nigeria.

<sup>2</sup>School of Engineering, Whittle Building, Cranfield University, Cranfield, Beds, MK43 0AL, UK.

<sup>a</sup>charles.o.woghiren@exxonmobil.com, <sup>b</sup>f.brennan@cranfield.ac.uk

**Keywords:** Tubular Joints, Stiffened Tubular Joints, Jack-up Platform, Multi Planar Tubular Joints, Welded Tubular Joints, Stress Concentration, Parametric Equations.

**Abstract** This paper reports a parametric stress analysis of various configurations of rack plate stiffened multi-planar welded KK joints using the finite element method. The KK joint finds application in the leg structure of offshore Oil & Gas jack-up platforms. The rack plate works as a stiffener which reduces the stress concentration at the brace/chord intersection. This could be an immense contribution to the increase in fatigue life of the joint, but other hot spot sites are introduced into the joint. The rack is also used for raising and lowering of the jack-up hull which gives the jack-up platform its jacking capability. Over one hundred and twenty models using a combination of shell and solid elements have been built and analysed with ABAQUS. Non-dimensional joint geometric parameters ( $\beta$ ,  $\gamma$  and  $\Omega$ ) are employed in the study, with the new parameter  $\Omega$  being defined as the ratio of rack thickness to chord diameter. Stress Concentration Factors (SCFs) are calculated under applied axial and OPB (out-of-plane-bending) loading. Three critical SCF locations are identified for each load case, with each location becoming the most critical based on the combination of the non-dimensional parameters selected for the joint. This is important as careful design can shift the critical SCF from an area inaccessible to NDT to one that can be easily inspected. The SCF values extracted from the models are used to derive six parametric equations through multiple regression analysis performed using MINITAB. The equations describe the SCF at the different locations as a function of the non-dimensional ratios. The equations not only allow the rapid optimisation of multi-planar joints but also can be used to quickly

identify the location of maximum stress concentration and hence the likely position of fatigue cracks. This in itself is an invaluable tool for planning NDT procedures and schedules.

## **1. Introduction**

Longitudinally stiffened tubulars find their greatest application in the legs of jack-up platforms. The stiffeners are usually found as rack plates which aid in the raising and lowering of the jack-up via a rack and pinion mechanism. A survey of available literature reveals that considerable research effort has been directed towards an understanding of the effect of internal ring stiffeners in tubular joints as opposed to the effect of longitudinal stiffeners, nevertheless the rack plate has been observed to reduce the stress concentration at the brace/chord intersection of stiffened joints. Stiffeners which reduce the stress concentration in certain locations are suspected of introducing hot spots in other locations and this justifies the need for research into the effect of rack plates in jack-up chords.

Extensive stress analyses of uni-planar tubular joints have been carried out in the past while most studies of multi-planar joints have focused on an ultimate strength analysis. Furthermore, study of the effect of stiffeners has mostly focused on their application to uni-planar joints. This parametric study involves a stress analysis of a rack plate stiffened multi-planar KK joint as shown in Figure 1.

The stiffened multi-planar KK joint under investigation is an integral part of the lattice legs of a jack-up platform as can be observed from Figure 2. Each leg is a critical component of the jack-up as failure of one leg will lead to the collapse of the whole structure. An extensive understanding of possible crack sites in the KK joint, which is to be achieved by this study, is a first step to prevent an eventual collapse of the platform.

A finite element analysis of over 120 models utilizing a combination of 3D solid elements and 2D shell elements was employed for the purpose of this work with the ultimate goal of developing parametric Stress Concentration Factor (SCF) equations to represent the hot spot stress at the brace/chord intersection and any other location identified as a potential hot spot.

The study has been restricted to axial and out-of-plane bending (OPB) loading modes while only three non-dimensional joint geometric parameters ( $\beta$ ,  $\gamma$  and  $\Omega$ ) were varied.

The circular chord in Figure 1 has been split to accommodate the continuous rack plate and is described as the opposed pinion leg configuration of a jack-up wherein the KK joint is repeated throughout the legs. Other leg configurations exist, but this study shall focus on the split tubular with a continuous central rack.

Consideration of in-plane bending (IPB) loads has been omitted from this study because of the negligible effect of the stiffener on the SCFs under IPB [1].

Other non-dimensional parameters to describe tubular joint geometry exist but the non-dimensional parameters selected for this study are believed to have the greatest effect on the SCFs in the joint under investigation.

## **2. Background**

The Jack-up Platform is better described as a Mobile Offshore Drilling Unit (MODU) and has been a part of the offshore oil industry exploration fleet since the 1950s. Many units in use today are over twenty years old which makes them very susceptible to fatigue failure.

The Jack-up was originally designed for intermittent use in shallow waters with periodic dry dock inspection and repair but the unit is re-usable as well as being simple and quick to install compared to fixed platforms, thus it finds increased application in the prolonged exploration of reservoirs in the harsher environments of deeper waters. This increased period of use implies less frequent inspection. Jack-ups are also being used as fixed production facilities, thus they are subjected to less frequent and expensive underwater inspection. This infrequent inspection requires that inspection schedules must be cost effective when carried out, possible locations of fatigue cracks must be identified and adequate mitigation measures employed.

Typical jack-up units consist of a buoyant triangular platform supported by three independent lattice legs, each resting on a large inverted conical footing known as a spud can. These are generally fabricated from High Strength weldable steel. High Strength Steel (HSS) bestows a high strength to weight ratio on the jack-up but is susceptible to Hydrogen Assisted Cracking (HAC) which is linked to the presence of welding defects, seabed Sulphate Reducing Bacteria (SRB) and the levels of applied cathodic protection [2].

The lattice legs of Jack-ups are a truss-work of chords, braces and span breakers (Figure 2). The braces provide the shear capacity of the legs while the chords provide the axial and flexural stiffness. The tubular members of the jack-up legs are joined in different configurations to produce T, Y, K or X joints in either uni-planar or multi-planar configurations. These joints are differentiated by the mode of load transfer exhibited.

Chiew *et al* [3] conducted a numerical and experimental stress analysis of a tubular XT joint and identified that the multi-planar effects in tubular joints can be categorised into multi-planar carry-over effects and multi-planar stiffness effects. The carry-over effect was attributed to the load interference to the in-plane brace members from the loading on the out-of-plane brace members and vice versa. The SCFs at the intersection of the in-plane brace members and the chord were described as carry-over SCFs. On the other hand, the presence of out-of-plane braces increases the total stiffness and load carrying capacity of the entire joint. This results in a decrease in the stress concentration at the loaded brace members and is described as the multi-planar stiffness effect. It was also observed that carry-over effects are negligible under IPB but become more pronounced under OPB and even to a greater extent under axial loads. In general it was concluded that the magnitude of the multi-planar effects depends on the load patterns and the relative geometrical locations of the brace members.

The lack of design guidelines for multi-planar joints in most codes results in a plane by plane assessment of the joints by designers, thus the effects of restraints and loads from other braces are ignored. Lee and Wilmsburst [4] identified that this practice can be either over conservative or grossly unsafe. Joop *et al* [5] proposed the application of a multi-planar

coefficient to the uni-planar joint capacity in order to estimate the ultimate strength of multi-planar joints. This approach was found to adequately account for the multi-planar effects in the joint.

Ramachandra *et al* [6] investigated the effect of internal ring stiffeners on the strength of tubular T and Y joints. The results of the experimental approach adopted for the problem revealed that the provision of three stiffeners in axially loaded T joints resulted in a 58.8% reduction of the maximum SCF in the chord and a 69.9% reduction in the brace. A 50% reduction was obtained in both the chord and the brace of an axially loaded Y joint. Lee and Llewelyn-Parry [7] utilised the finite element method for a problem similar to that investigated by Ramachandra but considered T and DT joints. Although internal ring stiffeners do not significantly affect the ductility of tubular joints they recommend that stiffeners positioned at the saddle position provide a better strength enhancement than those at the crown positions. The experimental investigation of Thandavamoorthy [8] revealed that bending of the chord of internally ring stiffened joints was the predominant mode of deformation as opposed to ovalising and punching shear of unstiffened joints.

A parametric study on the ultimate load carrying capacity of doubler plate reinforced T joints was executed by Chan *et al* [9]. A 150% increase in ultimate strength was observed for axially loaded joints while a 75% increase was observed for joints loaded in bending.

Myers *et al* [1] investigated the effect of rack plates on T and Y, in particular the influence on the SCF of three different longitudinal stiffeners. The constant thickness continuous stiffener returned the best performance when compared to the dual thickness stiffener (rack/rib plate) and the non-continuous stiffener. A 50% reduction in the maximum SCF was approached under axial loading, 20% reduction under out-of-plane bending while the peak SCF was unaffected by in-plane bending. The mechanism of operation of the longitudinal stiffener was observed to be the restraining of chord wall radial deformation, with thicker rack plates providing an additional restraint to chord deformation in the direction of the brace axis.

### 3. Scope and Definition of the Parametric Study

To ensure that the results of this study would be representative of the geometries found in practice an extensive review was conducted of Jack up joint geometries using the Noble Denton Rig Index [10] along with other information supplied by the Offshore Industry. A summary of this information is presented in Table 1.

Figure 3 depicts the grid of geometric parameters selected for the study as well as the load cases considered. Due to limitations in time and resources the study has been restricted to axial and out-of-plane bending (OPB) loading modes while only three non-dimensional joint geometric parameters ( $\beta$ ,  $\gamma$  and  $\Omega$ ) were varied.

The non-dimensional parameters ranges are:

$$0.3 \leq \beta \leq 0.54$$

$$4.62 \leq \gamma \leq 10$$

$$0.167 \leq \Omega \leq 0.467$$

Four values for each non-dimensional parameter were chosen roughly equally spaced in each parametric range giving a total of sixty-four possible combinations per load case and a total of one hundred and twenty-eight models would be employed for the parametric study. Other non-dimensional parameters were kept constant and all values defined for MSC CJ62 (upper bays) are given in Table 1.

Consideration of IPB was omitted from this study because of the negligible effect of the stiffener on the SCFs under such a load as reported by Myers *et al* [1]. The non-dimensional parameters selected for this study are believed to have the greatest effect on the SCFs for the stiffened multiplanar KK joint under investigation.

### 4. Finite Element Analysis of Multi-planar KK Joints

The parametric study was preceded by model validation analyses which successfully justified the boundary conditions and mesh refinement. The general effect of the longitudinal

stiffener was also investigated in that a reduction in the SCF was anticipated, hence an unstiffened full joint was analysed and compared with the stiffened full joint.

The complete details of a stiffened KK joint as found in MSC CJ62 (upper bays) are given in Table 2. The details of the FE mesh optimisation, refinement and convergence analyses can be found in reference [11]. In addition, several studies were conducted to verify the approach used against published solutions for uni-planar tubular joints [9, 12].

Element C3D20R from the ABAQUS family of 3D stress elements were used with reduced integration element control for meshing the joint area. This element is a 20 noded quadratic-brick element. Element S8R from the ABAQUS family of shell elements was used with reduced integration for meshing the shell section of the joint. It is an 8-noded doubly curved thick shell element with 6 degrees of freedom per node. In each case a convergence study was undertaken to optimise the mesh element density. An example of the results of one such study for the chord saddle SCF under axial tension is:

10	12	14	16	18	(Number of elements at brace/chord intersection)
5.574	5.555	5.517	5.505	5.502	(SCF)

To validate the technique, several related geometries were modelled and compared with results in the published literature. The results obtained were compared with Efthymiou and LR parametric equations as well as with the available SCF database [14]. An example of one such comparison for an unstiffened tubular T joint under axial and In-Plane Bending (IPB) is shown below:

Load Case	Efthymiou [14]	LR [14]	Database [14]	FEA
Axial	5.363	4.942	5.700	5.502
IPB	2.328	2.028	2.000	2.324

From the comparison above, it can be observed that the Efthymiou parametric equation [14] gives the best agreement with the present FEA results for all load cases and acceptable agreement with the LR equation and SCF database [14].

The stiffened model returned an internal SCF at the chord side of the chord/rack intersection under axial load. The rack plate appeared to have the following effects: it restrained the transverse deformation along the longitudinal axis and also reduced the radial deformation of the chord wall. The opposition to the radial deformation of the chord wall introduced by the rack plate created an internal tensile stress state which resulted in the internal SCF.

Figures 4 and 5 show stress contour plots of a stiffened KK joint under axial and OPB, respectively. Under OPB load, the hot spot occurred at the same location and the general mode of deformation remained similar to that for the unstiffened joint except that a lower SCF was observed for the stiffened case. The rack plate introduced some additional stiffness to the chord wall and hence resulted in the lower SCF.

## **5. Results and Discussion**

Three critical SCF locations were identified for each of the load cases investigated and suitable expressions to adequately describe the locations identified have also been established.

For the axial load study comprising sixty-four different models, the location of maximum stress concentration changed from model to model as the geometric parameters of the joint were varied. One internal SCF was observed in the vicinity of the chord/rack intersection while two external SCFs were noticed at the brace/chord intersection. For the OPB study, one internal SCF was observed in the vicinity of the brace/chord intersection, one external SCF at the chord/rack intersection and one external SCF at the brace/chord intersection.

A referencing system was adopted to identify the various SCF locations given as  $SCF_L-XYZ$ . Subscript 'L' represents the load case and X Y and z are given in Table 3.

### SCF Results for Axial Load

The internal SCF location identified under axial load is referred to as  $SCF_A-CRi$ . This indicates that an internal hot spot was observed at the chord side of the chord/rack intersection. Figure 6 shows a contour plot which indicates the location as  $SCF_A-CRi$ .

The external SCFs identified under axial load have respectively been referenced as  $SCF_A-BCc$  and  $SCF_A-CBs$ .  $SCF_A-BCc$  represents the external SCF observed at the crown heel on the brace side of the brace/chord intersection. An external hot spot was identified in between the saddle and crown but with greater proximity to the saddle. This location is referenced as  $SCF_A-CBs$  which indicates that the SCF was located on the chord side of the chord/brace intersection. Table 4 summarises the SCF results under axial load.

The following general observations can be made under axial load:

- The highest SCF is most likely found at an internal location in the vicinity of the chord/rack intersection;
- Low values of  $\beta$  produce low values of  $SCF_A-CRi$  and vice versa for high  $\beta$  values;
- Low values of  $\Omega$  favour high values of  $SCF_A-CRi$  while high values of  $\Omega$  result in low values of  $SCF_A-CRi$ ;
- As  $\gamma$  increases,  $SCF_A-CBs$  increases.

### SCF Results for OPB Load

The internal SCF location identified under OPB has been referenced as  $SCF_B-CBi$ . This indicates that an internal hot spot was observed at the chord side of the chord/brace intersection.

The external SCFs identified under OPB load have respectively been referenced as  $SCF_B-BCc$  and  $SCF_B-CRe$ .  $SCF_B-BCc$  represents the external SCF observed at the crown heel on the brace side of the brace/chord intersection. The external hot spot identified on the chord side of the chord/rack intersection has been referenced as  $SCF_B-CRe$ . Figure 7 shows a

stress contour plot indicating the location of SCF<sub>B</sub>–BCc, and Table 5 summarises the OPB results.

The following general observations can be made under OPB load:

- As  $\gamma$  increases, both SCF<sub>B</sub>–C<sub>Bi</sub> and SCF<sub>B</sub>–C<sub>Re</sub> increase;
- Low values of  $\beta$  favour low values of SCF<sub>B</sub>–C<sub>Re</sub> and vice versa for high  $\beta$  values.

### Validation of Results

There is little in the published domain to compare the results obtained. However, in order to gain confidence in the present results, a number of checks have been carried out:

- A detailed convergence study has been performed to ensure that the mesh used in the study reasonably represents the SCF obtained experimentally or in practice. The mesh adopted has been found to give good SCF results for a T joint when compared with parametric equations; by extension this mesh should have returned good results for the multi-planar joint.
- The effect of the stiffener in a T joint has been examined and it has been observed that ABAQUS [12] adequately captured the effect of the stiffener; by extension good results should have been obtained for the stiffened KK joint.

Although the additional braces in a multi-planar joint introduce some stiffening effects, Chiew *et al* [3] identified that the magnitude of the multi-planar effects depends on the load patterns and the relative geometrical locations of the brace members. It is assumed that for small values of  $\beta$  the stiffening effects would be minimized, thus the SCF in multi-planar joints with low  $\beta$  values can be compared with that in equivalent uni-planar joints. Parametric equations for unstiffened uni-planar K joints have been developed by Lloyds Register and are contained in HSE OTH 354 [14].

The rack plate should act to reduce the stress concentration at the brace/chord intersection, thus lower SCFs should be returned by the stiffened multi-planar KK joint when compared to an unstiffened uni-planar K joint of similar geometric configuration.

The only SCF that can be compared is the  $SCF_A-BCc$  as the Lloyds Register equations provide only saddle SCFs under OPB. No saddle SCF was obtained under OPB in this study and the SCF under axial load was not exactly at the saddle.

The results in Table 6 are as expected for  $\gamma$  values equal to 4.62 and 8. The results for  $\gamma$  equal to 6 and 10 return minor deviations from the expected results as the FEA results are slightly higher than those from LR equations. This deviation can be accepted because of the approximations in geometry of the joints being considered, also remembering that the FEA results for the unstiffened T joint were relatively higher than those predicted by the LR equation.

The results generally confirm that the stiffener acts to reduce the SCF at the brace/chord intersection, and the basis for comparing uni-planar joints with multi-planar joints can be taken to be acceptable.

## **6. Development of Parametric Equations**

The SCFs extracted from each model have been input into MINITAB [14] for regression purposes while the non-dimensional parameters have been supplied as predictor variables. The equations produced have been established by trial and error. The first sets of trials were aimed at achieving model equations with good fit and minimal deviation from the data points (SCFs). The six sets of SCFs extracted from the study have been found to display unique dependence on the non-dimensional parameters.

The industrial relevance of this study and the results obtained meant improvement iterations needed to be executed. These iterations required some trade-off between a good fit to the data and marginal over-prediction of the SCFs by the equations. The improvement was

achieved by assessing the performance of the initial equations and then marking up the FEA SCFs at all non-conservative points and marking down if required at conservative points. The regression analysis was then performed with the refined data.

It was observed that poor initial  $R^2$  values yielded quite difficult improvement iterations, nevertheless conservative SCFs are predicted by the new parametric equations. The final equations developed are given below.

$$SCF_A-CRi = -9.518 - 3.273\beta - 19.619\Omega + 12.240 \exp(\Omega) - 0.0321\gamma^2 + 1.86\beta\gamma + 14.892\beta\Omega + 0.368\gamma\Omega - 2.879\beta\gamma\Omega$$

$$SCF_A-BCc = 72.9 - 62\beta + 19.5\gamma - 2.60\Omega + 34\beta^{2.4} - 35.9\gamma^{0.85} + 3.37\Omega^2 - 49.6\gamma^{-1}\beta^{-1} + 6.90\gamma^{-1}\beta^{-2} + 8.8\beta\gamma^{0.85} - 7.0\beta^{2.4}\gamma^{0.85} + 5.35\gamma^{0.65}\beta^{12.5}\exp(-(\gamma - 10))$$

$$SCF_A-CBs = 3.50 - 2.11\Omega + 1.88\Omega^2 - 12.6\beta^{1.2}\gamma^{-1} + 0.0262(\beta^{-1.2}\gamma)\exp(\beta^{1.2}\gamma^{-1})$$

$$SCF_B-CRe = 0.798 - 5.056\beta - 0.207\gamma + 0.185\Omega + 1.405\beta\gamma$$

$$SCF_B-CBi = -0.972 + 2.81\beta + 0.443\gamma - 0.213\Omega - 0.811\gamma\beta^2 - 0.0168\gamma\beta^{-2}$$

The equations above are valid for the whole range of non-dimensional parametric values investigated (see Section 3).

It was impossible to fit a high quality equation to the entire database for  $SCF_B-BCc$ , hence a reduction in the validity range was imposed

$$SCF_B-BCc = 3.2 + 4.9\beta + 0.441\gamma - 3.4\exp(\beta) - 0.0714\beta^{0.6}\gamma^2 + 0.0327\gamma^{1.65}\beta^{24.5}\exp(-(\gamma - 20)) + 0.20\beta^2\Omega^2$$

$$0.3 \leq \beta \leq 0.54$$

$$4.62 \leq \gamma \leq 6$$

$$0.267 \leq \Omega \leq 0.467$$

The high values of  $R^2$  obtained indicate that good correlation exists between the predictor and response variables in the different SCF equations. The number of conservative points for the initial equations are about half of the total number of models considered. This implies that the equations gave a mean fit rather than a conservative fit.

After the improvement iterations have been performed, the final equations are conservative for more than 95% of the models analysed as can be inferred from Table 7. These equations still adopt the same predictor variables as the initial equations.

## 7. Conclusion

A systematic parametric study covering various configurations of a rack plate stiffened multi-planar KK joint has been executed using the finite element method. The KK joint under study finds application especially in the leg structure of jack-up platforms. The rack plate works as a stiffener which reduces the stress concentration at the brace/chord intersection, but other hot spot sites are introduced into the joint. The rack is also used for raising and lowering of the jack-up hull which gives the jack-up platform its peculiar jacking capabilities.

Over one hundred and twenty models using a combination of shell and solid elements have been built and analysed with ABAQUS. Non-dimensional joint geometric parameters ( $\beta$ ,  $\gamma$  and  $\Omega$ ) have been employed in the present study. Stress analyses of the joint when subjected to an axial load or to an OPB load have been performed.

The finite element procedure employed was verified by comparing the SCF results obtained against parametric SCF equations for unstiffened tubular joints, published in the available literature. The basis for this comparison was the assumption that, as the stiffener thickness and brace diameter decrease, the SCF for the joint under study should approach the SCF for the equivalent unstiffened joint. Acceptable correlation was obtained in all cases considered.

Three critical SCF locations were identified for each load case, with each location becoming the most critical based on the combination of the non-dimensional parameters selected for the joint. The SCF values extracted from the models have been used to derive six sets of parametric equations through multiple regression analysis performed using MINITAB. The equations describe the SCF at the different locations as a function of the non-dimensional ratios.

These equations have been produced for industrial application where safety and conservatism take precedence over a perfect fit of the equations to the data points. Several improvement iterations have therefore been performed in order to ensure that conservative SCFs are predicted by the equations. In all cases, the final equations are conservative for more than 95% of the models analysed.

The literature search carried out revealed very little information on the particular joint configuration studied, thus the critical SCF locations identified in this study could serve as a guide to future reliability based inspection planning for jack-up platforms. The number of non-dimensional parameters employed as well as the validity range of the equations produced makes the equations best suited for structural optimisation prior to any extensive design. These new design equations not only allow the rapid optimisation of multi-planar joints but also can be used to quickly identify the location of maximum stress concentration and hence the likely position of any fatigue cracks. This in itself is an invaluable tool for planning NDT procedures and schedules.

## **8. References**

- [1] Myers P T, Brennan F P and Dover W D, “The Effect of Rack/rib Plate on the Stress Concentration Factors in Jack-up chords”, *Marine Structures*, 14,485-505, 2001.
- [2] Sharp J V, Billingham J and Robinson M J, “The Risk Management of High Strength Steels in Jack-ups in Seawater”, *Marine Structures* 14, pp 537- 551, 2001.

- [3] Chiew, Sing-Ping, Soh, Chee-Kiong, Wu, Nai-Wen, “Experimental and Numerical Stress Analyses of Tubular XT-joint”, *Journal of Structural Engineering*, v 125, n 11, Nov, 1999, p 1239-1248.
- [4] Lee M.M.K and Wilmsburst S.R., “Parametric Study of Strength of Tubular Multi-planar KK Joints”, *Journal of Structural Engineering*, Vol. 122 No.8, August 1996.
- [5] Joop C.P, Yuji M and Yoshiaki K., “Ultimate Resistance of Unstiffened Multi-planar Tubular TT and KK Joints”, *Journal of Structural Engineering*, Vol. 120 No.10, October 1994.
- [6] Ramachandra D S, Gandhi P, Raghava G and Madhava Rao A G., “Fatigue Crack Growth in Stiffened Steel Tubular Joints in Seawater Environment”, *Engineering Structures* 22, pp 1390–1401, 2000.
- [7] Lee M M K and Llewelyn-Parry A, “Strength of ring-stiffened tubular T-joints in offshore structures —a numerical parametric study”, *Journal of Constructional Steel Research* 51, pp 239–264, 1999.
- [8] Thandavamoorthy T S, “Experimental Investigation on Internally Ring-stiffened Joints of Offshore Platforms”, *Structural Engineering Research Centre IE Journal* vol. 84, August 2003.
- [9] Chan T K, Fung T C, Tan C Y and Soh C K, “Behavior of Reinforced Tubular Joints”, *ICE proc. Issue 3*, pp 263 274, 2001.
- [10] Noble Denton Mobile Rig Index April 1992.
- [11] Woghiren, C. O., “Parametric SCF Study of Longitudinally Stiffened Tubulars”, MSc Thesis, University College London, 2006.
- [12] Brennan F P, Peleties P and Hellier A K, “Predicting Weld Toe Stress Concentration Factors for T and Skewed T-Joint Plate Connections”, *Int. J of Fatigue* pp 573-584, 2000.
- [13] ABAQUS Version 6.4-4. Hibbit, Karlson and Sorensen Inc.
- [14] Lloyd’s Register of Shipping, “Stress Concentration Factors for Simple Tubular Joints; Assessment of existing and development of new parametric formulae”, HSE OTH 354 1997.

[15] MINITAB Release 14 Statistical Software. Minitab Inc, 3081 Enterprise Drive, State Collge, PA 16801, USA.

Design	L1	z	D	L	T	$\Omega$	d	$l_b$	t	$\alpha$	$\beta$	$\tau$	$\gamma$
F&G L780 (lower bays)	400	152	381		25	0.399							7.62
F&G L780 (upper bays)	400	127	381		25	0.333							7.62
F&G L780 m2 (lower bays)	400	152	381	3658	32	0.399	219	4343	24	19.20	0.57	0.75	5.95
F&G L780 m2 (upper bays)	400	127	381	3658	32	0.333	219	4343	18	19.20	0.57	0.56	5.95
F&G L780 m5 (monitor)	401	178	381		81	0.467							2.35
F&G L780 m5 (monarch)	401	178	381		81	0.467							2.35
F&G L780 m6	611	178	584		83	0.305							3.52
MSC CJ62 (lower bays)	650	210	600	6927	65	0.350	324	7700	30	23.09	0.54	0.46	4.62
MSC CJ62 (upper bays)	650	210	600	6927	55	0.350	324	7700	28	23.09	0.54	0.51	5.45
MSC CJ50 (1)	550	210	520		25	0.404							10.40
MSC CJ50 (2)	550	210	520		25	0.404							10.40
MSC CJ46 (1)	540	150	520		50	0.288	273		14		0.53	0.28	5.20
MSC CJ46 (2)	540	150	520		25	0.288	273		14		0.53	0.56	10.40
Technip TPG 500 (1)	722	160	680		75	0.235							4.53
Technip TPG 500 (2)	722	160	680		75	0.235							4.53
Technip TPG 500 (3)	722	160	680		62	0.235							5.48
Technip TPG 500 (4)	722	160	680		58	0.235							5.86
Technip TPG 500 (5)	722	160	680		50	0.235							6.80
Technip TPG 500 (6)	722	160	680		50	0.235							6.80

Source: Noble Denton Rig Index [10] all dimensions in mm

L1 = rack root-root distance; L = chord length;  $\alpha = 2L/D$ ;  $l_b$  = brace length; t = brace thickness;  $\tau = t/T$

Table 1: Database of jack-up joint configurations

Parameter	Magnitude	Description
D	600mm	Chord diameter
d	324mm	Brace diameter
T	55mm	Chord thickness
t	28mm	Brace thickness
L1	650mm	Rack root-root distance
Z	210mm	Rack thickness
G	500mm	Gap between braces
L	4500mm	Chord length
$l_b$	2250mm	Brace length
$\Theta$	66°	inclination of brace to chord
B	0.54	$d/D$
$\Gamma$	5.45	$D/2T$
$\Omega$	0.35	$z/D$
A	15	$2L/D$
$\tau$	0.51	$t/T$

Table 2: Geometric parameters of KK joint

L	X	Y	z
A - Axial	B – Brace	B – Brace	c - crown
B - OPB	C – Chord	C – Chord	e – external
	R - Rack	R - Rack	i – internal
			s - saddle

Table 3: SCF Referencing System

Model ID No.	$\Omega$	$\gamma$	$\beta$	SCF <sub>A</sub> -CRi	SCF <sub>A</sub> -BCc	SCF <sub>A</sub> -CBs	Peculiarity to the study
KAXL-131-017	0.167	8	0.3	2.989	3.180	3.106	All values approx. equal
KAXL-144-031	0.167	10	0.54	<b>5.925</b>	2.993	3.025	Highest SCF <sub>A</sub> -CRi
KAXL-441-121	0.467	10	0.3	<b>1.921</b>	3.262	3.411	Lowest SCF <sub>A</sub> -CRi
KAXL-121-009	0.167	6	0.3	2.984	<b>3.601</b>	2.660	Highest SCF <sub>A</sub> -BCc
KAXL-434-119	0.467	8	0.54	4.246	<b>2.142</b>	2.319	Lowest SCF <sub>A</sub> -BCc
KAXL-241-057	0.267	10	0.3	2.274	3.369	<b>3.620</b>	Highest SCF <sub>A</sub> -CBs
KAXL-314-071	0.367	4.62	0.54	3.993	2.897	<b>1.596</b>	Lowest SCF <sub>A</sub> -CBs

Table 4: Summary of SCFs under axial load

Model ID No.	$\Omega$	$\gamma$	$\beta$	SCF <sub>B</sub> -CRe	SCF <sub>B</sub> -BCc	SCF <sub>B</sub> -CBi	Peculiarity to the study
KOPB-431-114	0.467	8	0.3	0.929	0.954	1.165	All values approx. equal
KOPB-231-050	0.267	8	0.3	0.909	0.942	1.169	All values approx. equal
KOPB-144-032	0.167	10	0.54	<b>3.291</b>	1.036	1.893	Highest SCF <sub>B</sub> -CRe
KOPB-111-002	0.167	4.62	0.3	<b>0.224</b>	1.143	0.656	Lowest SCF <sub>B</sub> -CRe
KOPB-133-022	0.167	8	0.5	1.436	<b>1.810</b>	1.704	Highest SCF <sub>B</sub> -BCc
KOPB-134-024	0.167	8	0.54	2.015	<b>0.878</b>	1.582	Lowest SCF <sub>B</sub> -BCc
KOPB-143-030	0.167	10	0.5	3.077	1.040	<b>2.091</b>	Highest SCF <sub>B</sub> -CBi
KOPB-411-098	0.467	4.62	0.3	0.299	1.184	<b>0.634</b>	Lowest SCF <sub>B</sub> -CBi

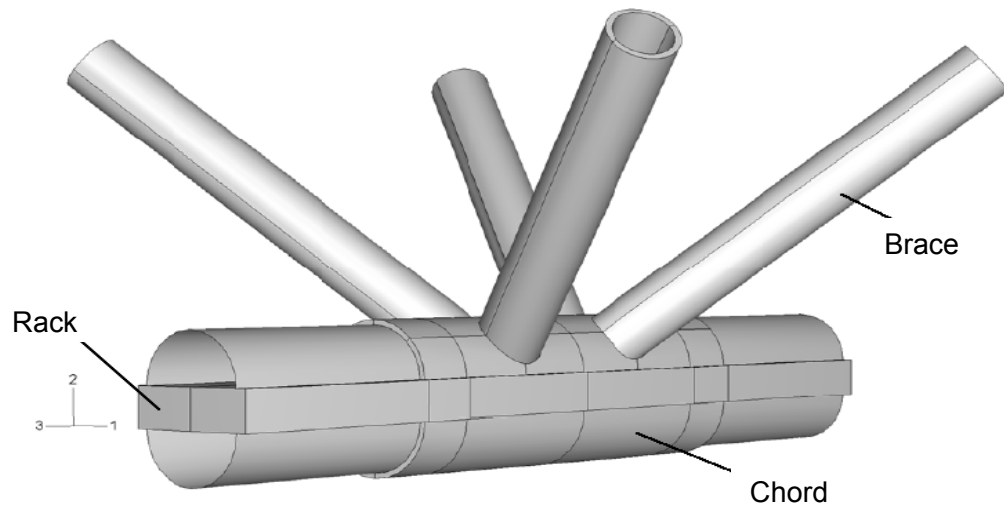
Table 5: Summary of SCFs under OPB load

Model ID No	$\Omega$	$\gamma$	B	FEA (multi-planar KK)	LR (uni-planar K)
KAXL-111-001	0.167	4.62	0.3	3.042	3.540
KAXL-211-033	0.267	4.62	0.3	3.049	3.540
KAXL-311-065	0.367	4.62	0.3	2.967	3.540
KAXL-411-097	0.467	4.62	0.3	3.003	3.540
KAXL-121-009	0.167	6	0.3	3.601	3.416
KAXL-221-041	0.267	6	0.3	3.520	3.416
KAXL-321-073	0.367	6	0.3	3.489	3.416
KAXL-421-105	0.467	6	0.3	3.452	3.416
KAXL-131-017	0.167	8	0.3	3.180	3.351
KAXL-231-049	0.267	8	0.3	3.066	3.351
KAXL-331-081	0.367	8	0.3	3.031	3.351
KAXL-431-113	0.467	8	0.3	3.013	3.351
KAXL-141-025	0.167	10	0.3	3.460	3.383
KAXL-241-057	0.267	10	0.3	3.369	3.383
KAXL-341-089	0.367	10	0.3	3.336	3.383
KAXL-441-121	0.467	10	0.3	3.262	3.383

Table 6: Comparison of  $SCF_A$ -BCc with LR equations [14]

Initial Analysis						
SCF	$SCF_A$ -CRi	$SCF_A$ -BCc	$SCF_A$ -CBs	$SCF_B$ -CRe	$SCF_B$ -CBi	$SCF_B$ -BCc
$R^2$	0.976	0.929	0.839	0.981	0.987	0.889
MSE	0.0199	0.0135	0.0440	0.0160	0.0021	0.0029
Conservative Points	31	28	31	23	27	12
Improvement Iteration						
% Mark-up	10	18	32	24	14.5	20
% Mark-down	0	-3.7	-3.2	0	0	0
MSE	0.110	0.183	0.451	0.092	0.022	0.028
Cp	-	-	4.5	5	6	1.5
Conservative Points	63	60	62	61	61	24
Data Points	64	64	64	64	64	24

Table 7: Parametric Fit Characteristics



$D$  = chord diameter

$z$  = rack thickness

$d$  = brace diameter

$T$  = chord wall thickness

$$\Omega = z/D$$

$$\beta = d/D$$

$$\gamma = D/2T$$

Figure 1: 3D view of stiffened KK joint.

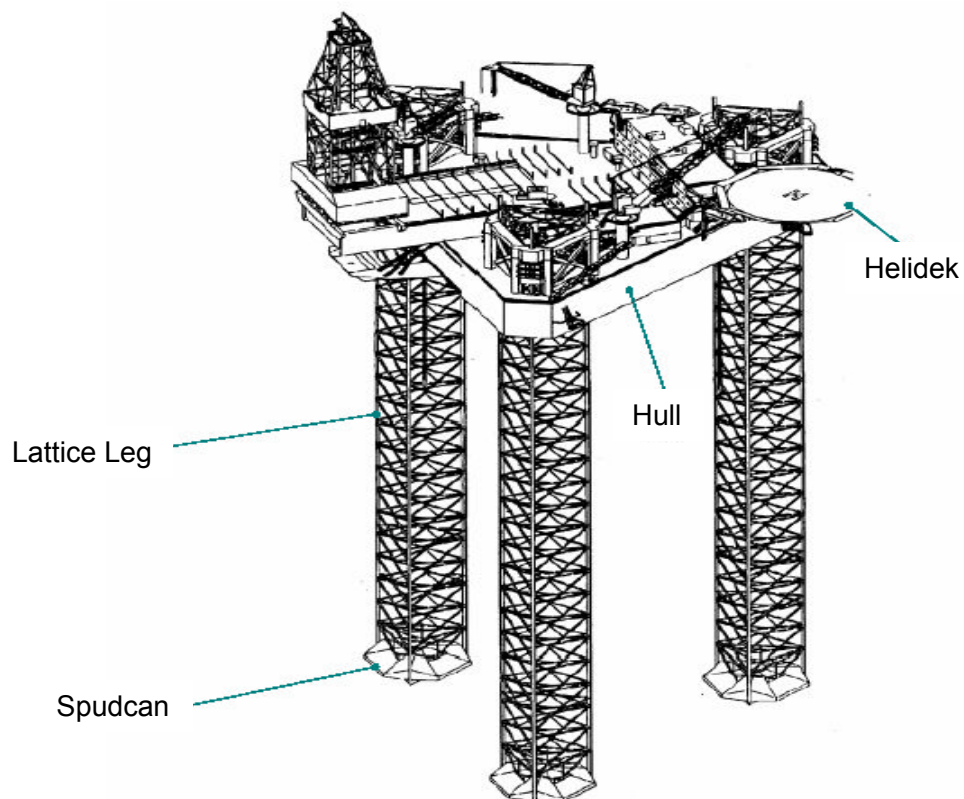


Figure 2: General view of a jack-up

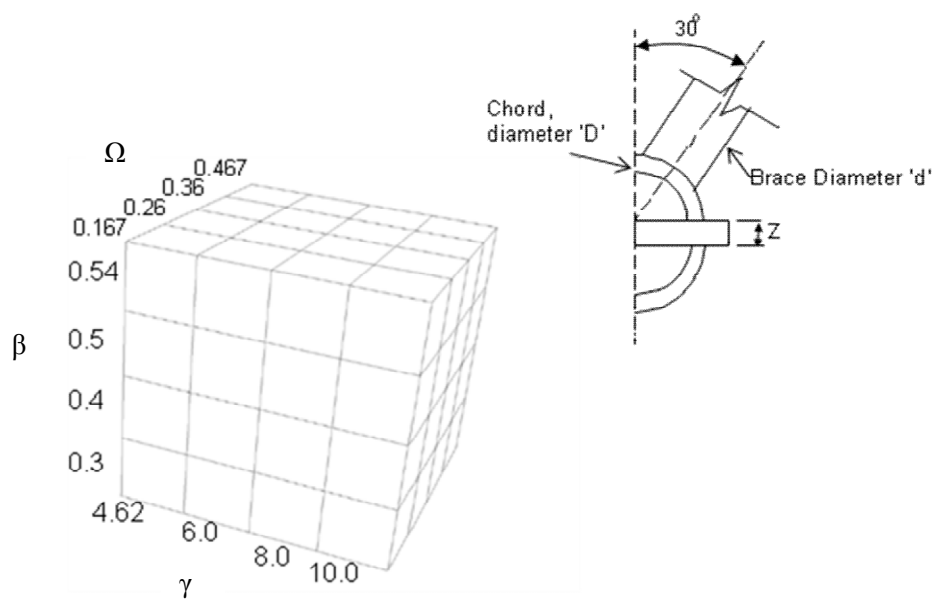


Figure 3: Parametric matrix of FE models.

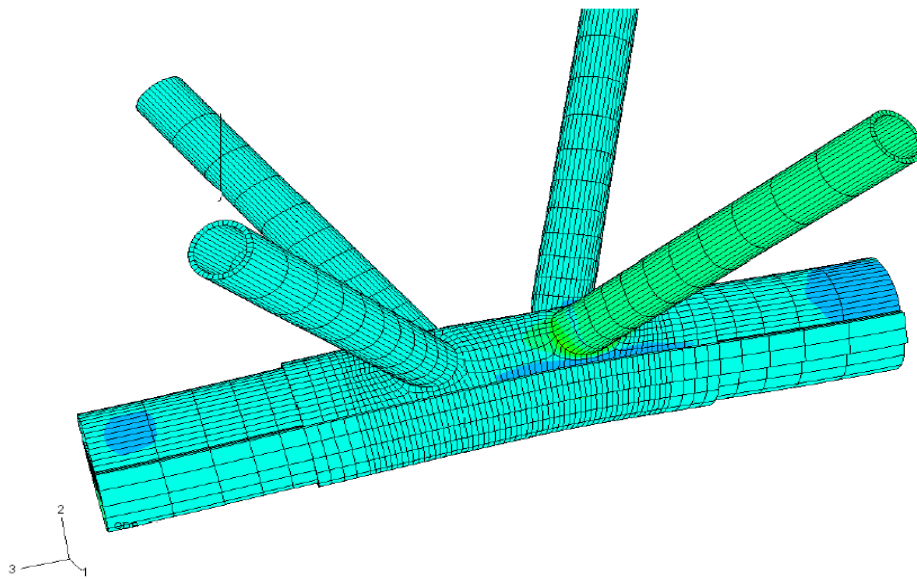


Figure 4: Stress contour plot of a stiffened KK joint under axial tension

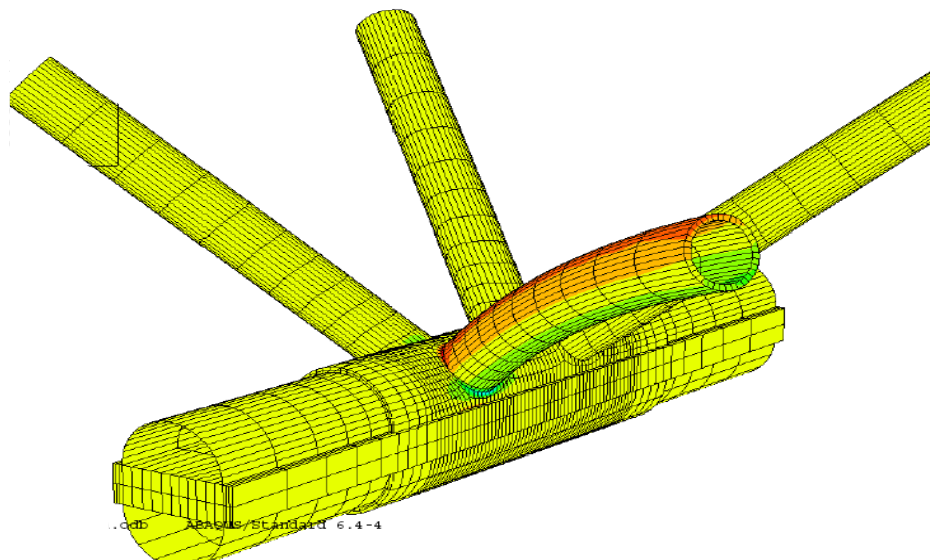


Figure 5: Stress contour plot of a stiffened KK joint under OPB

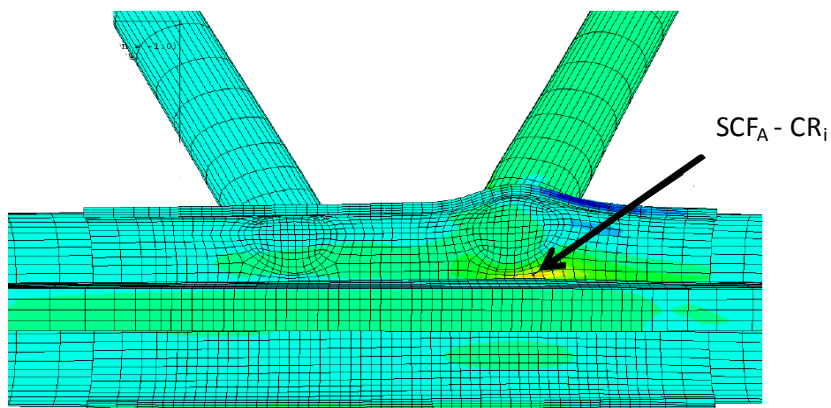


Figure 6: Stress contour plot indicating the location of  $SCF_A - CR_i$

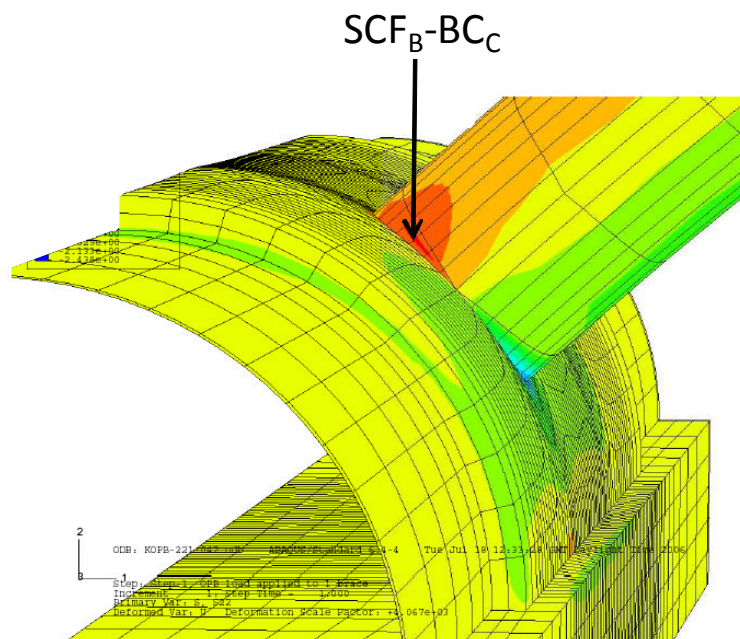


Figure 7: Contour plot indicating the location of  $SCF_B - BC_c$

# Weld toe stress concentrations in multi-planar stiffened tubular KK joints

Woghiren, C. O.

2009-01-31T00:00:00Z

---

C. O. Woghiren and F. P. Brennan. Weld toe stress concentrations in multi-planar stiffened tubular KK joints. International Journal of Fatigue, Volume 31, Issue 1, January 2009, Pages 164-172

<http://dx.doi.org/10.1016/j.ijfatigue.2008.03.039>

*Downloaded from CERES Research Repository, Cranfield University*